Hierarchical sliding mode control and disturbance observer for the double inverted pendulum on a cart

Nguyen Thi Van Anh*, Nguyen Duy Hung, Tran Huu Phuoc,
Nguyen Danh Huy, Nguyen Tung Lam

Hanoi University of Science and Technology, Hanoi, Vietnam.
*Corresponding author: anh.nguyenthivan1@hust.edu.vn.
Received 29 Jun. 2023; Revised 21 Sep. 2023; Accepted 10 Nov. 2023; Published 25 Nov. 2023.
DOI: https://doi.org/10.54939/1859-1043.j.mst.91.2023.35-44

ABSTRACT

This paper presents a control approach for the double inverted pendulum on a cart (DIPC) by combining Hierarchical Sliding Mode Control (HSMC) and Disturbance Observer (DOB). The proposed method utilizes HSMC to ensure balance in both the pendulum angles and a cart position, while the DOB accurately estimates the system's disturbance. Through the simulations, the integrated HSMC and DOB approach demonstrates remarkable efficacy in achieving stable equilibrium control of the double inverted pendulum. Comparative analysis against the commonly used Linear Quadratic Regulator (LQR) controller highlights the superior performance and efficiency of our proposed method.

Keywords: Double inverted pendulum; Disturbance observer; Hierarchical sliding mode control; Linear quadratic regulator.

1. INTRODUCTION

Over the past years, there has been a growing focus on the control of underactuated systems, driven by their diverse applications in numerous scientific and technological domains. A particularly intriguing system that has attracted substantial research attention is the Double Inverted Pendulum on Cart (DIPC) control [1-3]. The DIPC system comprises two pendulums interconnected in an inverted configuration, characterized by nonlinear dynamics and inherent instability, which present significant control design challenges. Achieving effective control of the DIPC system holds immense importance across various fields, including robotics [4], where the ability to stabilize and manipulate such systems is crucial for the development of advanced robotic platforms. Similarly, in aerospace engineering, precise and stable control of similar systems can enhance the performance and maneuverability of unmanned aerial vehicles and spacecraft. The inherent complexity and instability of the DIPC system make it an intriguing platform for exploring and developing innovative control strategies and algorithms, with the goal of attaining robust stability and efficient control performance. Consequently, extensive research efforts have been dedicated to devising control approaches that can effectively address the unique challenges posed by the DIPC system, paving the way for advancements in control theory and practical applications.

In the realm of control strategies for the Double Inverted Pendulum on Cart (DIPC), various approaches have been explored, including optimal control [5], fuzzy control [6], and Linear Quadratic Regulator (LQR) [7]. However, among these methods, hierarchical sliding mode control (HSMC) [8, 9] has emerged as a particularly promising and effective approach for achieving stability in the DIPC system. HSMC utilizes a hierarchical structure and multiple sliding surfaces to confine the system's trajectory within desired stability boundaries. Its robustness against uncertainties and disturbances makes it an ideal choice for addressing the inherent challenges posed by the DIPC system. Unlike other

control strategies, HSMC prioritizes stability control rather than tracking performance, making it well-suited for achieving stable control of the DIPC system.

This paper presents a novel approach that leverages HSMC to enhance the control quality of the DIPC, specifically considering the presence of disturbances. HSMC is a sophisticated control technique that integrates multiple sliding surfaces and control rules to improve overall system performance and stability. By employing a hierarchical structure, HSMC offers several advantages, including enhanced control accuracy, reduced chattering effects, and increased stability in the face of external disturbances. Furthermore, the integration of a disturbance observer (DOB) [10] plays a crucial role in effectively estimating and compensating for disturbances within the control process. This ensures system stability, reliability, and improved resistance to disturbances and unexpected variations encountered in real-world environments.

The proposed approach holds great promise for achieving robust stability control in the DIPC system, offering a viable solution to the challenges associated with its nonlinear and unstable nature. Through simulations and empirical evaluations, the effectiveness of the HSMC-based control method is demonstrated, and a comparative analysis is conducted against the conventional LQR control approach. The findings underscore the superior performance of HSMC in terms of stability, control quality, and disturbance rejection, further validating its potential as an advanced control strategy for the DIPC system.

2. DIPC MODELING

In this paper, we consider the DIPC model, as depicted in figure 1. In the system, we define the following parameters: m_0, m_1, and m_2 represent the masses of the cart, first pendulum, and second pendulum respectively. L_1 and L_2 denote the lengths of the first and second pendulums respectively. The variable x_0 represents the position of the cart, while θ_1 and θ_2 represent the angular positions of the first and second pendulums respectively. J_1 and J_2 represent the moments of inertia of the first and second pendulums respectively. Additionally, g represents the acceleration due to gravity, and u represents the force to be applied to the cart.

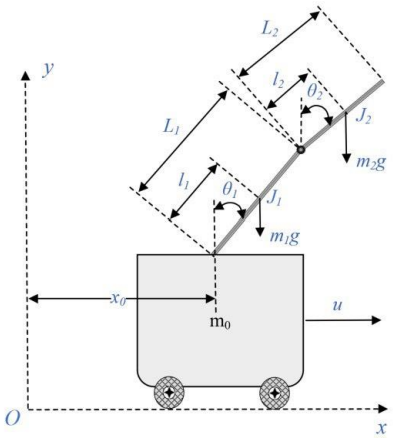

Figure 1. *DIPC Model.*

The system is modeled using the Lagrange equation. L represents the Lagrange function with $\theta = \begin{bmatrix} x_0 & \theta_1 & \theta_2 \end{bmatrix}^T$; $U = \begin{bmatrix} u & 0 & 0 \end{bmatrix}^T$.

$$\frac{d}{dt}\left(\frac{\partial L}{\partial \dot{\theta}}\right) - \frac{\partial L}{\partial \theta} = U. \tag{1}$$

The Lagrange function can be written as follows:

$$\begin{aligned} L = {} & \frac{1}{2}a_1\dot{x}_0^2 + \frac{1}{2}a_4\dot{\theta}_1^2 + \frac{1}{2}a_6\dot{\theta}_2^2 + a_2 cos(\theta_1)\dot{x}_0\dot{\theta}_1 + a_3 cos(\theta_2)\dot{x}_0\dot{\theta}_2 \\ & + a_5 cos(\theta_1 - \theta_2)\dot{\theta}_1\dot{\theta}_2 - a_2 g cos\theta_1 - a_3 g cos\theta_2 \end{aligned} \tag{2}$$

where a_1, a_2, a_3, a_4, a_5, a_6 are constants.

$$a_1 = m_0 + m_1 + m_2;\ a_2 = m_1 l_1 + m_2 L_1;\ a_3 = m_2 l_2;$$
$$a_4 = m_1 l_1^2 + m_2 L_1^2 + I_1;\ a_5 = m_2 L_1 l_2;\ a_6 = m_2 l_2^2 + I_2.$$

The dynamic equation for the DIPC can be written in matrix form:

$$D(\theta)\ddot{\theta} + C(\theta, \dot{\theta})\dot{\theta} + G(\theta) = Hu. \tag{3}$$

where

$$D(\theta) = \begin{pmatrix} a_1 & a_2 cos\theta_1 & a_3 cos\theta_2 \\ a_2 cos\theta_1 & a_4 & a_5 cos(\theta_1 - \theta_2) \\ a_3 cos\theta_2 & a_5 cos(\theta_1 - \theta_2) & a_6 \end{pmatrix};\ G(\theta) = \begin{pmatrix} 0 \\ -a_2 g sin\theta_1 \\ -a_3 g sin\theta_2 \end{pmatrix};$$

$$C(\theta, \dot{\theta}) = \begin{pmatrix} 0 & -a_2 sin(\theta_1)\dot{\theta}_1 & -a_3 sin(\theta_2)\dot{\theta}_2 \\ 0 & 0 & a_5 sin(\theta_1 - \theta_2)\dot{\theta}_2 \\ 0 & -a_5 sin(\theta_1 - \theta_2)\dot{\theta}_1 & 0 \end{pmatrix};\ H = (1\,0\,0)^T.$$

3. CONTROL DESIGN

In this section, we delve into the control strategies employed for the DIPC system. We explore three distinct approaches: LQR control, HSMC, and the implementation of a DOB. By studying these control strategies, we aim to evaluate their effectiveness in achieving stability of the DIPC system, considering the disturbance factor.

3.1. LQR Control

By examining equation (3), the following equation can be readily obtained:

$$\ddot{\theta} = -D^{-1}C\dot{\theta} - D^{-1}G + D^{-1}Hu. \tag{4}$$

$$\Rightarrow \begin{cases} \ddot{x}_0 = f_1(x_0, \dot{x}_0, \theta_1, \dot{\theta}_1, \theta_2, \dot{\theta}_2, u) \\ \ddot{\theta}_1 = f_2(x_0, \dot{x}_0, \theta_1, \dot{\theta}_1, \theta_2, \dot{\theta}_2, u) \\ \ddot{\theta}_2 = f_3(x_0, \dot{x}_0, \theta_1, \dot{\theta}_1, \theta_2, \dot{\theta}_2, u) \end{cases} \tag{5}$$

Denote:

$$p_1 = x_0;\ p_2 = \dot{x}_0;\ p_3 = \theta_1;\ p_4 = \dot{\theta}_1;\ p_5 = \theta_2;\ p_6 = \dot{\theta}_2. \tag{6}$$

Subsequently, we obtain:

$$\dot{p}_1 = p_2 = \dot{x}_0;\ \dot{p}_2 = f_1;\ \dot{p}_3 = p_4 = \dot{\theta}_1;\ \dot{p}_4 = f_2;\ \dot{p}_5 = p_6 = \dot{\theta}_2;\ \dot{p}_6 = f_3. \tag{7}$$

In the case of the DIPC, the desired operating point is determined as follows:

$$p_d = \begin{bmatrix} p_{1d} & p_{2d} & p_{3d} & p_{4d} & p_{5d} & p_{6d} \end{bmatrix}^T = \begin{bmatrix} 0 & 0 & 0 & 0 & 0 & 0 \end{bmatrix}^T \tag{8}$$

By linearizing the nonlinear system around the working point, we obtain an equation of the form:

$$\dot{p} = A.p + B.u \tag{9}$$

with

$$p = \begin{bmatrix} p_1 \\ p_2 \\ p_3 \\ p_4 \\ p_5 \\ p_6 \end{bmatrix},\ A = \begin{bmatrix} 0 & 1 & 0 & 0 & 0 & 0 \\ A_{11} & A_{12} & A_{13} & A_{14} & A_{15} & A_{16} \\ 0 & 0 & 0 & 1 & 0 & 0 \\ A_{21} & A_{22} & A_{23} & A_{24} & A_{25} & A_{26} \\ 0 & 0 & 0 & 0 & 0 & 1 \\ A_{31} & A_{32} & A_{33} & A_{34} & A_{35} & A_{36} \end{bmatrix},\ B = \begin{bmatrix} 0 \\ B_{11} \\ 0 \\ B_{21} \\ 0 \\ B_{31} \end{bmatrix}$$

and $A_{jz} = \left.\frac{\partial f_j}{\partial p_z}\right|_{\substack{u=0 \\ p=0}};\ B_{j1} = \left.\frac{\partial f_j}{\partial u}\right|_{\substack{u=0 \\ p=0}};\ j = 1,2,3;\ z = 1,2,3,4,5,6.$ Next, we define the weight matrices for the states and control variables in the following manner: $R = \begin{bmatrix} R_1 \end{bmatrix}$; $Q = diag\{Q_1, Q_2, Q_3, Q_4, Q_5, Q_6\}$. The control signal of the LQR exhibits the following form:

$$u = -K.p \tag{10}$$

where $K = R^{-1}(B^T P + N^T)$. P can be calculated through the Riccati function: $A^T P + PA - (PB + N)R^{-1}(B^T P + N^T) + Q = 0.$ In all cases, to simplify the Riccati function we choose $N = 0$. K is calculated using Matlab with the command: $K = lqr(A, B, Q, R).$

3.2. Hierarchical Sliding Mode Control

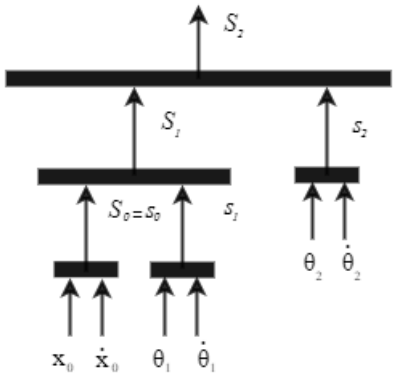

Figure 2. *HSMC controller structure.*

In this subsection, we explore the HSMC approach for controlling the DIPC system in the presence of disturbances. The HSMC controller utilizes multiple sliding surfaces to address the control objectives. The HSMC method involves partitioning the DIPC system into three subsystems: two inverted pendulums and the cart. The hierarchical structure of the HSMC controller, illustrating the interaction between these subsystems, is depicted in figure 2.

We have:

$$\begin{bmatrix} \ddot{x}_0 & \ddot{\theta}_1 & \ddot{\theta}_2 \end{bmatrix}^T = \begin{bmatrix} M_0 & M_1 & M_2 \end{bmatrix}^T + \begin{bmatrix} N_0 & N_1 & N_2 \end{bmatrix}^T u \tag{11}$$

where $\begin{bmatrix} M_0 & M_1 & M_2 \end{bmatrix}^T = -D^{-1}(C\dot{\theta} + G);\ \begin{bmatrix} N_0 & N_1 & N_2 \end{bmatrix}^T = D^{-1}H.$

By setting the desired output value x_{0d}, θ_{1d}, θ_{2d}, we obtain:

$$e_0 = x_{0d} - x_0;\ e_1 = \theta_{1d} - \theta_1;\ e_2 = \theta_{2d} - \theta_2. \tag{12}$$

For the subsystems, the sliding surfaces are selected as follows:

$$s_0 = \lambda_0 e_0 + \dot{e}_0;\ s_1 = \lambda_1 e_1 + \dot{e}_1;\ s_2 = \lambda_2 e_2 + \dot{e}_2. \tag{13}$$

Then

$$\dot{s}_i = \lambda_i \dot{e}_i + \ddot{e}_i = \lambda_i \dot{e}_i + \ddot{\theta}_{id} - (M_i + N_i u). \tag{14}$$

Denote $\dot{s}_i = 0$, we have:

$$u_{eqi} = \frac{\lambda_i \dot{e}_i + \ddot{\theta}_{id} - M_i}{N_i} \tag{15}$$

where the control signals u_{eqi} $(i = 0,1,2)$ are utilized to drive the subsystems towards stabilization on their respective sliding surfaces. The hierarchical sliding surface can be represented as follows:

$$S_0 = s_0;\ S_1 = \varepsilon_0 S_0 + s_1;\ S_2 = \varepsilon_1 S_1 + s_2. \tag{16}$$

where ε_0, ε_1 are positive constants. In order for the subsystems to achieve stability on their respective sliding surfaces, the overall control signal must incorporate sub-control signals. As a result, the control signal for the entire system takes the following form:

$$u = u_{eq0} + u_{eq1} + u_{eq2} + u_{sw} \tag{17}$$

where u_{sw} enables the system to slide on a specified sliding surface. Choose a Lyapunov function of the form $V = S_2^{\,2}/2$. The derivative of V combined with the equations (13) and (16) we get: $\dot{V} = S_2 \dot{S}_2 = S_2\left(\varepsilon_1\left(\varepsilon_0\left(\lambda_0 \dot{e}_0 + \ddot{e}_0\right) + \left(\lambda_1 \dot{e}_1 + \ddot{e}_1\right)\right) + \left(\lambda_2 \dot{e}_2 + \ddot{e}_2\right)\right)$. By combining equations (11), (12), (15), and (17), we obtain the following expression:

$$\dot{V} = S_2\left(\varepsilon_1\left(\varepsilon_0\left(-N_0(u_{eq1} + u_{eq2} + u_{sw})\right) + (-N_1(u_{eq0} + u_{eq2} + u_{sw})\right) + (-N_2(u_{eq0} + u_{eq1} + u_{sw})\right)$$

Denote $\dot{S}_2 = -\eta sign(S_2)$, we have:

$$u_{sw} = -\frac{\varepsilon_1\varepsilon_0 N_0\left(u_{eq1}+u_{eq2}\right)}{\varepsilon_1\varepsilon_0 N_0+\varepsilon_0 N_1+N_2} - \frac{\varepsilon_0 N_1\left(u_{eq0}+u_{eq2}\right)}{\varepsilon_1\varepsilon_0 N_0+\varepsilon_0 N_1+N_2} - \frac{N_2\left(u_{eq0}+u_{eq1}\right)}{\varepsilon_1\varepsilon_0 N_0+\varepsilon_0 N_1+N_2} + \frac{\eta sign(S_2)}{\varepsilon_1\varepsilon_0 N_0+\varepsilon_0 N_1+N_2}.$$

Hence the control signal is obtained as follows

$$u = u_{eq0}+u_{eq1}+u_{eq2}+u_{sw} = \frac{\varepsilon_1\varepsilon_0 N_0 u_{eq0}+\varepsilon_0 N_1 u_{eq1}+N_2 u_{eq2}+\eta sign(S_2)}{\varepsilon_1\varepsilon_0 N_0+\varepsilon_0 N_1+N_2}. \quad (18)$$

To ensure system stability, it is required that $\eta > 0$.

3.3. Disturbance observer

The DIPC model has the form:

$$\ddot{\theta} = -a\dot{\theta} + bu - c - d \quad (19)$$

with $\theta = [x_0\ \theta_1\ \theta_2]^T$, $a = D^{-1}C$, $b = D^{-1}H$, $c = D^{-1}G$, d is the disturbance. Next, we introduce the concept of the disturbance observer :

$$\dot{\bar{d}} = \alpha_1(\bar{v} - \dot{\theta});\ \dot{\bar{v}} = -\bar{d} + bu - \alpha_2(\bar{v} - \dot{\theta}) - a\dot{\theta} - c. \quad (20)$$

where $\bar{d}$ is estimated disturbance, $\bar{v}$ is the matrix with dimension 3×1 related to the estimated velocity of the cart, the first pendulum and the second pendulum. α_1, α_2 are positive matrices.

Select the Lyapunov function as follows:

$$V = \frac{1}{2\alpha_1}e_d^{\,2} + \frac{1}{2}e_v^{\,2} \quad (21)$$

with $e_d = d - \bar{d}$, $e_v = \dot{\theta} - \bar{v}$. By taking the derivative of V, we obtain: $\dot{V} = \frac{1}{\alpha_1}e_d\dot{d} - \alpha_2 e_v^{\,2} \le 0$. To ensure that $\dot{V} \le 0$, the values of α_1 and α_2 must be sufficiently large. After constructing the DIPC model, HSMC and disturbance observer, the overall structure used for simulation is depicted in figure 3.

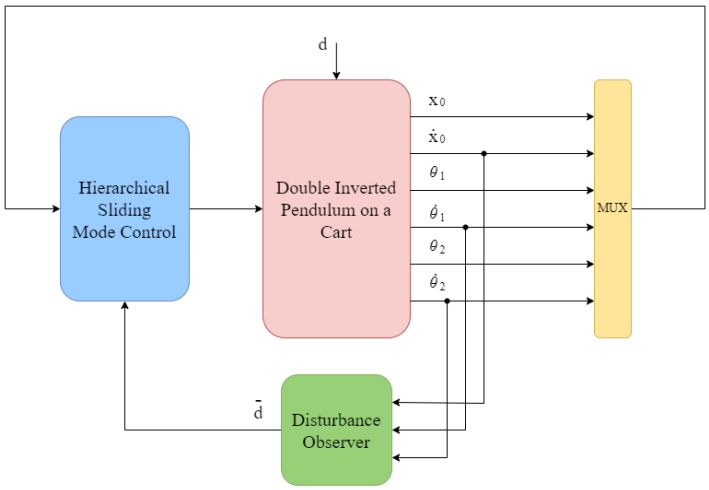

Figure 3. *HSMC and DOB control structure.*

4. SIMULATION RESULTS

To verify the performance of the controller, the DIPC system was evaluated using the following set of parameters: $m_0 = 0.8\ Kg$; $m_1 = 0.5\ Kg$; $m_2 = 0.3\ Kg$; $L_1 = 0.3\ m$; $L_2 = 0.3\ m$; $J_1 = 0.006\ Kg.m^2$; $J_2 = 0.006\ Kg.m^2$; $g = 9.8\ m/s^2$. At the initial stage, we have the following initial conditions: x_0=0 m; $\dot{x}_0$=0 m/s; $\theta_1 = \pi/6$ rad; $\dot{\theta}_1 = 0$ rad/s; $\theta_2 = \pi/6$ rad; $\dot{\theta}_2 = 0$ rad/s. For HSMC and disturbance observer, there are some paramaters: $\lambda_0 = 1.1$; $\lambda_1 = 0.1$; $\lambda_2 = 2.8$; $\varepsilon_0 = 3$; $\varepsilon_1 = 0.25$; $\alpha_1 = [4000 \quad 1000 \quad 500]$; $\alpha_2 = [50 \quad 50 \quad 50]$; $a = [0]_{3\times3}$; $b = [0.8 \quad 0.1 \quad 0.1]^T$, note that all the elements in a matrix is zero due to the desired operating point value. To evaluate the performance of the controller in the presence of disturbance, the cart is subjected to disturbance of the following form: $d = 0.1\sin(t)$. Figures 4 to 7 present the verification results for the aforementioned control algorithms. It is evident that the HSMC controller exhibits a smaller steady-state oscillation amplitude. However, during the transition phase, the HSMC controller requires a larger control signal of 300 N, in comparison to the LQR controller which only needs 37 N.

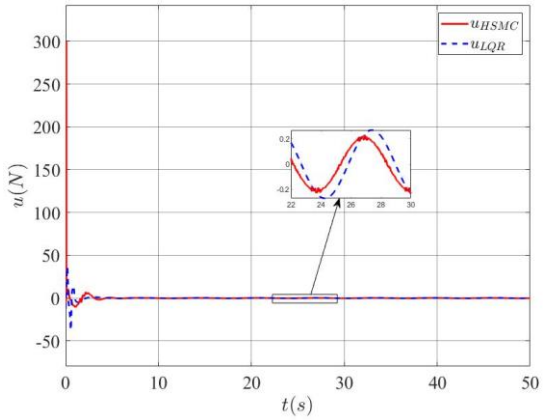

Figure 4. *HSMC and LQR control signals.*

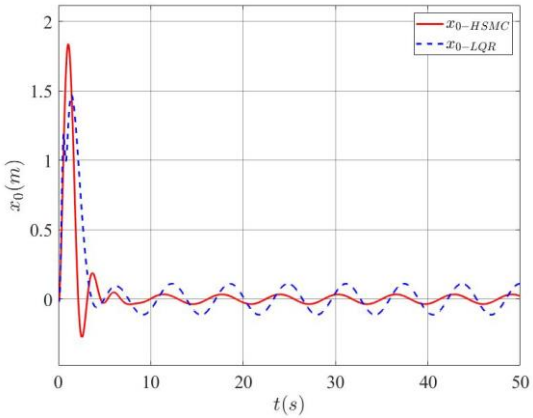

Figure 5. *Comparison of Cart Position between HSMC and LQR Controllers.*

In figure 5, it can be observed that the HSMC controller demonstrates a higher overshoot, with the farthest position reaching 1.83 m and an oscillation amplitude of 0.05 m, whereas the LQR controller achieves a maximum position of 1.47 m with an oscillation amplitude of 0.11 m.

Figure 6 illustrates the comparison of the angle of the first pendulum between the two controllers. The LQR method yields a maximum rotation angle of 0.7 rad, which is greater than that achieved by the HSMC method, which is 0.5 rad. Moving on to the angle of the second pendulum, as depicted in figure 7, it is evident that the HSMC method results in a larger maximum angle of 0.42 rad, while the LQR method produces a maximum rotation angle of 0.3 rad for the second pendulum.

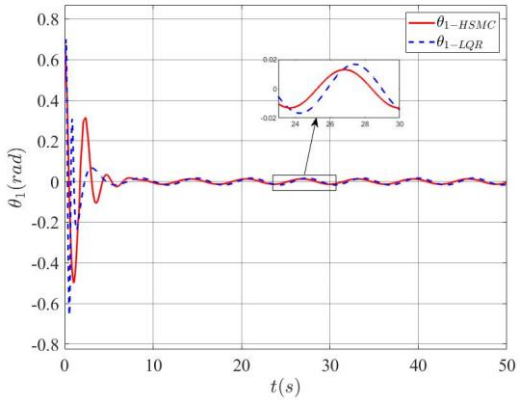

Figure 6. *Comparison of the first pendulum Angle between the Two Controllers.*

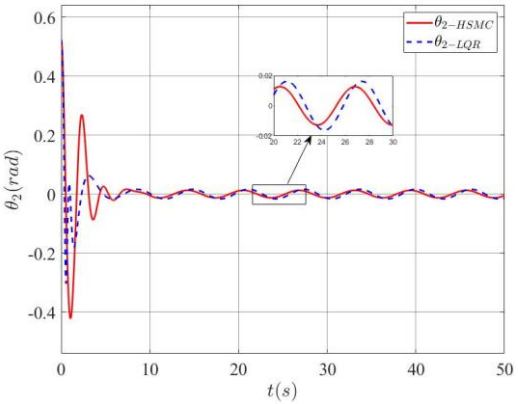

Figure 7. *Comparison of the second pendulum Angle between the Two Controllers.*

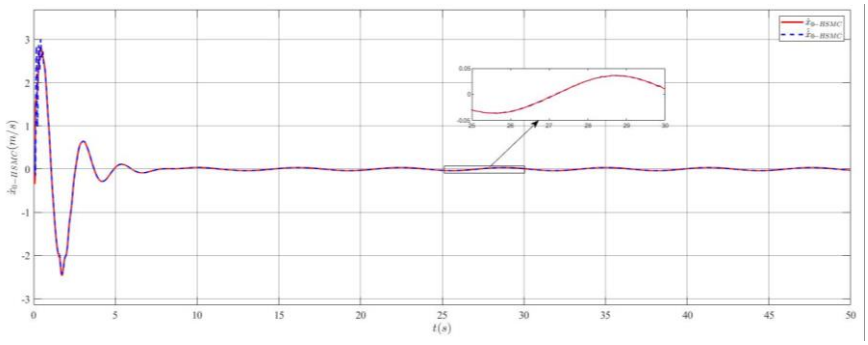

Figure 8. *Comparison between practical Cart Velocity and estimated Cart Velocity.*

Figures 8, 9, 10 depict the comparison between the practical and estimated values of cart velocity, first pendulum angle velocity, and second pendulum angle velocity when using HSMC controller, respectively. It is evident that the estimated values closely follow the practical values and there is a deviation between them because of the presence of disturbance.

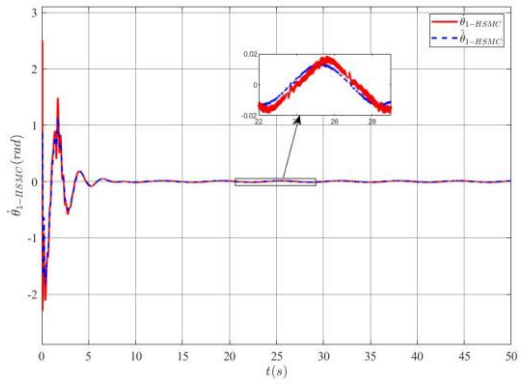

Figure 9. *Comparison between the practical Velocity of the first pendulum and the estimated Velocity of the first pendulum.*

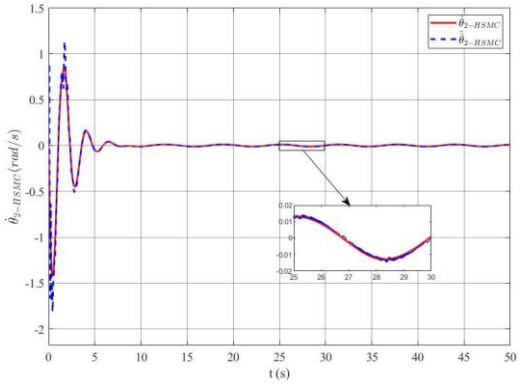

Figure 10. *Comparison between the practical Velocity of the second pendulum and the estimated Velocity of the second pendulum.*

Figures 11 and 12 demonstrate the performance of the disturbance observer when controlled by the HSMC and LQR methods. It is evident that observer stabilization is more effective when utilizing the LQR method for controlling the DIPC. On the other hand, the HSMC method introduces chattering, which affects the performance of the disturbance observer. During the transient phase, the maximum estimated disturbance value for the LQR method is significantly larger, reaching a maximum of 46, compared to the HSMC method, which yields a maximum estimated noise value of 13.

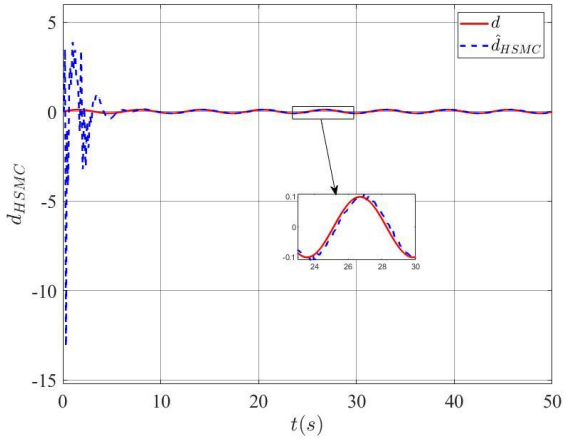

Figure 11. *Comparison of disturbance and estimated disturbance when controlled by HSMC.*

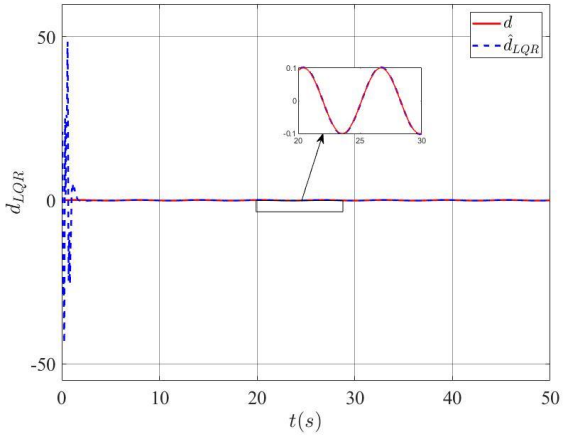

Figure 12. *Comparison of disturbance and estimated disturbance when controlled by LQR.*

5. CONCLUSIONS

This paper presented a comparative study of HSMC and LQR controllers for the DIPC system. The results showed that the HSMC controller exhibited superior performance in terms of smaller steady-state oscillations and reduced overshoot. However, it was also observed that the HSMC controller introduced chattering, while the LQR controller provided better observer stabilization and estimation of disturbance. These findings highlight the trade-offs between control effectiveness and stability in different control methods for the DIPC system. Further research could focus on addressing the chattering issue in HSMC or exploring hybrid control approaches to harness the strengths of both methods for improved control performance.

REFERENCES

[1]. Tijani, Tunde Mufutau, and Isah Abdulrasheed Jimoh. *"Optimal control of the double inverted pendulum on a cart: A comparative study of explicit MPC and LQR."* Applications of Modelling and Simulation 5: 74-87, (2021).

[2]. Habib, Maki K., and Samuel A. Ayankoso. *"Modeling and Control of a Double Inverted Pendulum using LQR with Parameter Optimization through GA and PSO."* 2020 21st International Conference on Research and Education in Mechatronics (REM). IEEE, (2020).

[3]. Nejadfard, Atabak, Mohammad Javad Yazdanpanah, and Iraj Hassanzadeh. *"Friction compensation of double inverted pendulum on a cart using locally linear neuro-fuzzy model."* Neural Computing and Applications 22: 337-347, (2013).

[4]. Magdalena, S. Żurawska, Maksymilian Szumowski, and Teresa Zielińska. *"Reconfigurable double inverted pendulum applied to the modelling of human robot motion."* Journal of Automation, Mobile Robotics and Intelligent Systems: 12-20, (2017).
[5]. Bogdanov, Alexander. *"Optimal control of a double inverted pendulum on a cart."* Oregon Health and Science University, Tech. Rep. CSE-04-006, OGI School of Science and Engineering, Beaverton, OR (2004).
[6]. Cheng, Fuyan, et al. *"Fuzzy control of a double-inverted pendulum."* Fuzzy sets and systems 79.3: 315-321, (1996).
[7]. Yadav, Sandeep Kumar, Sachin Sharma, and Narinder Singh. *"Optimal control of double inverted pendulum using LQR controller."* International Journal of Advanced Research in Computer Science and Software Engineering 2.2 (2012).
[8]. Qian, Dianwei, Jianqiang Yi, and Dongbin Zhao. *"Hierarchical sliding mode control for a class of SIMO under-actuated systems."* Control and cybernetics 37.1: 159-175, (2008).
[9]. Qian, Dianwei, et al. *"Hierarchical sliding mode control for series double inverted pendulums system."* 2006 IEEE/RSJ International Conference on Intelligent Robots and Systems. IEEE, (2006).
[10]. Liu, Jinkun, et al. *"Advanced sliding mode control"*. Springer Berlin Heidelberg, pp. 206-217, (2011).

TÓM TẮT

Điều khiển trượt tầng HCMC và quan sát nhiễu cho hệ thống con lắc ngược đôi trên xe

Bài báo này trình bày một phương pháp kết hợp bộ điều khiển trượt tầng (Hierarchical sliding mode control - HSMC) và bộ quan sát nhiễu (Disturbance Observer) để điều khiển con lắc ngược đôi trên xe. Bộ điều khiển trượt tầng được sử dụng để điều khiển cân bằng cho các góc của con lắc ngược đôi và vị trí của xe. Trong khi đó, bộ quan sát nhiễu được sử dụng để ước lượng nhiễu tác động lên hệ thống. Kết quả mô phỏng đạt được từ việc kết hợp các phương pháp trên đã mang lại hiệu quả cao trong việc điều khiển con lắc ngược đôi ổn định tại trạng thái cân bằng. Kết quả này đã được chứng minh được sự vượt trội hơn khi so sánh với bộ điều khiển Linear Quadratic Regulator (LQR).

Từ khoá: Con lắc ngược đôi trên xe; Điều khiển ổn định; Điều khiển trượt tầng; Điều khiển LQR; Bộ quan sát nhiễu.